AIP | Applied Physics Letters

High temperature terahertz response in a p-type quantum dot-in-well photodetector

Seyoum Wolde, Yan-Feng Lao, A. G. Unil Perera, Y. H. Zhang, T. M. Wang, J. O. Kim, Ted Schuler-Sandy, Zhao-Bing Tian, and S. Krishna

Citation: Applied Physics Letters **105**, 151107 (2014); doi: 10.1063/1.4898088
View online: http://dx.doi.org/10.1063/1.4898088
View Table of Contents: http://scitation.aip.org/content/aip/journal/apl/105/15?ver=pdfcov
Published by the AIP Publishing

High temperature terahertz response in a *p*-type quantum dot-in-well photodetector

Seyoum Wolde,[1] Yan-Feng Lao,[1] A. G. Unil Perera,[1,a)] Y. H. Zhang,[2] T. M. Wang,[2] J. O. Kim,[3] Ted Schuler-Sandy,[3] Zhao-Bing Tian,[3] and S. Krishna[3]
[1]*Department of Physics and Astronomy, Georgia State University, Atlanta, Georgia 30303, USA*
[2]*Key Laboratory of Artificial Structures and Quantum Control, Department of Physics and Astronomy, Shanghai Jiao Tong University, Shanghai 200240, China*
[3]*Center for High Technology Materials, Department of Electrical and Computer Engineering, University of New Mexico, Albuquerque, New Mexico 87106, USA*

(Received 28 July 2014; accepted 1 October 2014; published online 14 October 2014)

Terahertz (THz) response observed in a *p*-type InAs/$In_{0.15}Ga_{0.85}As$/GaAs quantum dots-in-a-well (DWELL) photodetector is reported. This detector displays expected mid-infrared response (from ~3 to ~10 μm) at temperatures below ~100 K, while strong THz responses up to ~4.28 THz is observed at higher temperatures (~100–130 K). Responsivity and specific detectivity at 9.2 THz (32.6 μm) under applied bias of −0.4 V at 130 K are ~0.3 mA/W and ~1.4×10^6 Jones, respectively. Our results demonstrate the potential use of *p*-type DWELL in developing high operating temperature THz devices. © *2014 AIP Publishing LLC*. [http://dx.doi.org/10.1063/1.4898088]

The advances of research and technology in the quantum dot infrared photodetector (QDIP) have attracted much attention for the mid-wave and long-wave infrared applications.[1,2] A variety of studies have reported that QDIPs are capable of operating at elevated temperatures,[2–4] which, however, typically leads to device operation responding in the mid-wave infrared regime. The development of Terahertz (THz) sources[5] and progress required terahertz detectors. One of the difficulties lies in the absorption of THz radiation corresponding to very small energy, which is typically about 4.1–41 meV (1–10 THz), below the range of thermal energy for temperatures ~300 K (25.8 meV). The dark current at the temperature, as high as 77 K is dominant over the photocurrent in the lower energy range of THz detection. As a consequence, THz devices are very sensitive to temperature variation and are usually unable to operate at high temperatures. For instance, most of the terahertz detectors in the range of ~3–10 THz operate at low temperatures (4.6 K to 80 K).[6–8] In this letter, we report a *p*-type THz dot-in-well (DWELL) detector with a response up to ~4.28 THz (~70 μm) operating at 130 K.

Most detectors with DWELL structures are based on the intersubband transitions from ground state of the QD to an excited state close to the barrier or GaAs band edge.[7,9] The bound to continuum transitions have an escape probability of ~100% for photoexcited carriers and leads to a high photocurrent at lower bias. On the other hand, due to better wave function overlap between the two states, the bound to bound transitions have better absorption coefficients, but lower escape probability at lower biases. For any THz detector, the transition energy between the two states should fall in the THz energy range of 4.1–41 meV (1–10 THz). To match the excited state with the continuum and having the energy spacing between the states in the terahertz region, the width and height of the well, and the size and shape of the QD have to be adjusted. The ground and excited state energies can be tuned by changing width and height of the well. However, in practice, size of QD is very limited due to the inability to make the dot size as desired in Stranski-Krastanov (SK) growth mode.[10] An alternative approach for small energy spacing in terahertz QD based detector is *p*-type-doped structure, which has higher density of states as compared to its *n*-type counterpart. Moreover, at a given temperature, the higher effective mass of holes in the valence-band will result in lower holes transport as compared to the electrons in conduction band and, consequently, a reduction in dark current.[11,12]

Most of the THz investigations thus far have been with *n*-type QDIP and used resonant tunneling[13] or dark current blocking layers.[10] Using dark current blocking layers, an *n*-type Tunneling quantum dot photodetector (T-QDIP) operating at 150 K with spectral response up to ~55 μm (Ref. 13) and a Quantum ring detector operating at 120 K with spectral responses up to ~30 μm have been reported.[8] So far, little or no attention has been paid to *p*-type DWELL structures responding in the THz region. Therefore, the motivation of this work is to achieve THz *p*-type DWELL detection up to ~4.28 THz (~70 μm) at operating temperature of 130 K or higher.

In this study, we report a THz DWELL detectors based on *p*-type intersubband transition, where the InAs dots are placed in $In_{0.15}Ga_{0.85}As$, which in turn is positioned in a GaAs matrix as shown in Fig. 1(a). The measured responsivity shows that as the temperature changes from ~100 K to 130 K, the longer wavelength (>14 μm) responses increase, while mid-infrared (MIR) responses decrease. Comparison of the calculated hole energy levels in QD as shown in Fig. 1(b) with the measured spectral response shows that the MIR response peak at ~5.4 μm corresponds to transition of holes from the ground state to the continuum. The THz response at high temperature is attributed to the transitions from the excited state to quasi-bound state or continuum. The probability of occupying exciting states increases with increasing temperature. The excited states have a higher

a)uperera@phy-astr.gsu.edu

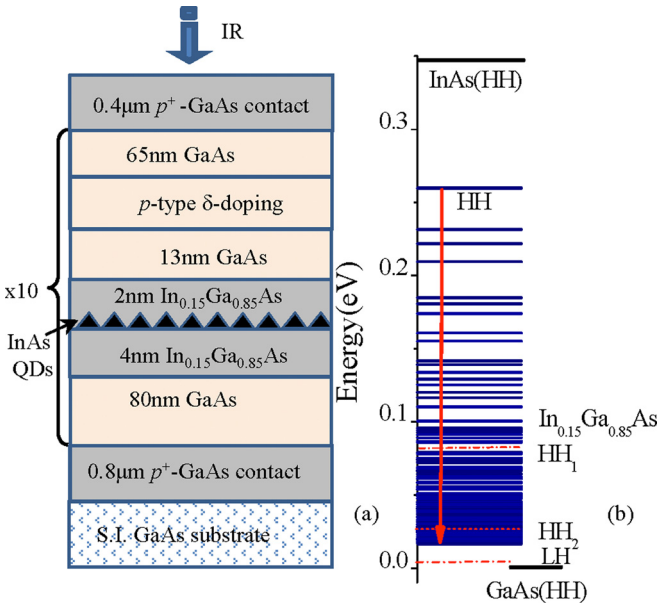

FIG. 1. (a) Schematic diagram for *p*-type DWELL structure of InAs QDs embedded in $In_{0.15}Ga_{0.85}As$ QW. (b) QD valence band structure calculated with an eight-band **k·p** model[15] and the QW states are computed using effective mass method.[16] The spin orbital split-off energy (SO) levels are intentionally omitted for the reason that transitions to SO levels fall in short wavelength region, which are not our primary focus. The dashed lines are the two HH and LH states for $In_{0.15}Ga_{0.85}As$ QW. Transitions can be either from bound to bound or from bound to quasi-bound (or continuum) energy level. The MIR absorption in Fig. 1(b) is due to transition from ground state to continuum state, while the THz transitions are possibly from bound to quasi-bound or continuum states.

degeneracy than the ground state. Hence, despite the low occupation probability, the total number of carriers in excited states is comparable to that of the ground states at higher temperatures.[14] Furthermore, for the same incident power, there are more photons at 32.6 μm than at 5.4 μm. Therefore, as the temperature increases from ~100 K to 130 K, due to broadening of Fermi-Dirac distribution, carriers will have appreciable concentrations at higher energy levels and result in the THz response.

The detector structure shown in Fig. 1(a) is grown by molecular beam epitaxy (MBE), consists of 10 stacks of DWELL structures sandwiched between two highly doped p^+-GaAs contact layers, grown on a semi-insulating GaAs substrate. The active region contains InAs QDs placed in 6 nm thick $In_{0.15}Ga_{0.85}As$ quantum well (QW), which in turn is surrounded by GaAs barrier layers. The dot density is about $5 \times 10^{10}\,cm^{-2}$. A δ-doping technique is used, with a sheet density of $5 \times 10^{11}\,cm^{-2}$ *p*-type dopants placed above the QWs (with a 13 nm thick GaAs spacer), which introduces about 10 free holes in each QD. The QDs have nearly pyramidal shape with the average base widths of ~20–25 nm and height of ~5 nm.[7] The devices were fabricated into square mesas of $400 \times 400\,\mu m^2$ with an optical window of $260 \times 260\,\mu m^2$, which allows front-side illumination. In order to characterize the device, the square mesas and the ohmic contacts on the top and bottom layers were fabricated using standard wet chemical etching. Then, the device was mounted on the cold head of the liquid nitrogen-cooled dewar and liquid helium-cooled cryostat to allow measurements of spectral response, noise, and dark current. The normal incidence spectral response was measured using a Perkin-Elmer system 2000 Fourier transform infrared spectrometer. A bolometer with known sensitivity was used for background measurements and measured data were corrected by the background spectra.

An eight-band **k·p** model was used to calculate QD hole states with the effects of strain included with the valence force field model,[15] whereas the QW levels were calculated using the effective-mass method.[16] As shown in Figure 1(b), the QW was designed to have two heavy holes (HH) with almost continuous set of QD HH and light hole (LH) levels. Therefore, DWELL detectors represent a hybrid of quantum well infrared photodetector (QWIP) and QDIP.[17] Hole transitions can be either from bound to bound or from bound to quasi-bound (or to the continuum).

The spectral responses were measured over temperature range from 78 K to 130 K. The 5.4 μm (0.230 eV) peak corresponds to hole transition from the ground state of QD to states near the GaAs barrier.[18] At 78 K, holes lie in the ground states which lead to the main response peak in the MIR range. The elevated temperature results in the broadening of Fermi distribution function and more carriers occupying the upper energy states where the energy spacing is in the order of THz energy range. Hence, the corresponding bound-to-continuum or quasi bound transition results in THz response and increases with temperature. Figure 2(a) shows clearly the comparison of MIR and THz responses at three different bias values. The THz response spectra start to appear for temperatures higher than ~100 K, which is featured with a broad spectral range over ~70 μm. Although detection of terahertz radiation up to 1 THz could be expected due to closely spaced upper energy states, the background noise level due to high dark current dominates the

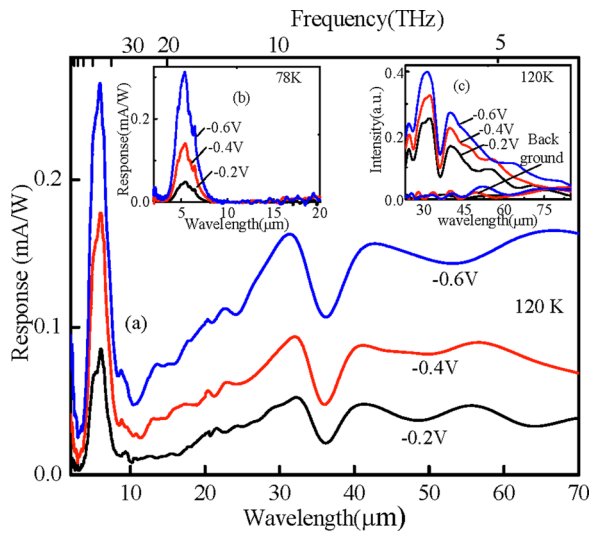

FIG. 2. (a) Responsivity versus wavelength measured at T = 120 K for three different bias values. (b) Response versus wavelength measured at T = 78 K. This response is due to the transitions from ground state of QD to states near the GaAs band edge. Unlike the response spectra of (a), (b) has only one peak in MIR region. There are no low energy transitions or THz response at 78 K. (c) Comparison of raw data of THz response and background noise level. The THz response spectra are broad and extend beyond ~70 μm. The lower energy response (lower than 17.7 meV or ~70 μm) is below back ground noise level.

photocurrent at wavelength higher than 70 μm as shown in Figure 2(c).

Variation of MIR and THz response spectra with temperature at a fixed applied bias of −0.4 V (or field of ∼1.89 kV/cm) is shown in Figure 3. The THz response increases with increasing temperature, which contrasts with decreasing MIR peak at higher temperatures. For a temperature increase from 80 K to ∼90 K, the response increases reaching the highest response at ∼90 K. In QD holes are confined due to energy quantization in all three dimensions and electron-hole scattering is greatly reduced.[19] Since the intersubband energy between ground state and continuum is larger than phonon energy, the optical phonon emission is not allowed. As a result, the hole relaxation time from the continuum states increases due to phonon bottle neck.[19] This increase in response with the temperature may be related to reduced relaxation of carriers back to QD from the continuum states[4] and to enhanced escape of excited carriers. As the temperature is further increased, due to decrease in carrier concentration of ground state and increase carrier population in excited states, MIR response starts to decrease and THz response starts to appear. In the temperature ranges (∼100 to 130 K) where we see the THz response, MIR response decreases with increasing temperature.

Furthermore, it is experimentally confirmed that the THz region (or the broad response peak) starts to appear only for temperatures beyond ∼100 K and increases as the temperature rises from 100 K to 130 K. The calculated energy spacing between the dot levels varies from ∼5 meV to 28 meV. There is no peak shift with either bias voltage or temperature. The dark current increases from 2.4×10^{-3} A/cm^2 to 0.12 A/cm^2, which is about 50 times increase for temperature changes from 100 to 130 K. At 130 K and −0.6 V bias, the thermal noise calculated from equation $I_{th} = \sqrt{4KT/R}$, where K is Boltzmann constant, T is temperature, and R is differential resistance of device is 1.18×10^{-12}A/$\sqrt{\text{Hz}}$ and the corresponding shot noise $I_d^n = \sqrt{2eI_d}$ is 7.1×10^{-12} A/$\sqrt{\text{Hz}}$, which is close to the measured noise current of 7.5×10^{-12}A/$\sqrt{\text{Hz}}$ indicating the dominant role of dark current noise at a temperature of 130 K. From 78 K to 130 K, the peak responsivity of the 5.4 μm absorption peak decreases by ∼65%, while the responsivity of much longer wavelengths around the ∼32.6 μm absorption peak increases by a factor of ∼100 as the temperature changes from 100 K to 130 K. Hence, it can be said that the THz response possibly originates from thermal excitation of carriers in QD states and is strongly temperature dependent. The longer wavelength (∼32.6 μm) response was measured at the highest temperature of 130 K with peak responsivity of ∼0.54 mA/W (at an applied bias of −0.6 V), which is a very high operating temperature as compared to THz QW and QD detectors.[7,20] Moreover, using a high-speed mid-IR photoconductivity technique, long carrier lifetimes 3–600 ns in an InAs/ $In_{0.15}Ga_{0.85}As$ DWELL heterostructures have been observed suggesting their potential for high temperature operation[21] and have promise for fabrication of long wave-length infrared (LWIR) imaging focal plane arrays (FPA).[22] DWELL structure can also reduce the thermionic emission by lowering the ground state of the dot with respect to the GaAs band edge, and enables the detector to operate on transitions from the ground state of InAs QD to a state in the InGaAs QW.[9] Hence, by optimizing the doping level and well width of DWELL for longer carrier life time or higher escape probability, detector responses and detectivity can be improved and extend the THz detection with operating temperature up to 130 K or higher.

Figure 4(a) shows the dark current density versus voltage characteristics for temperature in the range of 80–130 K. As the temperature increases from 70 K to 150 K, the dark current density increased sharply from 7.8×10^{-7} A/cm^2 to 0.26 A/cm^2 at −0.2 V and from 6.34×10^{-6} to 0.62 A/cm^2 at −0.6 V, which are still lower than the dark current values of other IR device operating at lower or the same temperature in a comparable wavelength region.[8,13,23] At lower temperatures, the increase in dark current density with applied bias was due mainly to the lowering of the potential barriers. In the Arrhenius plot shown in Figure 4(b), the dark current to

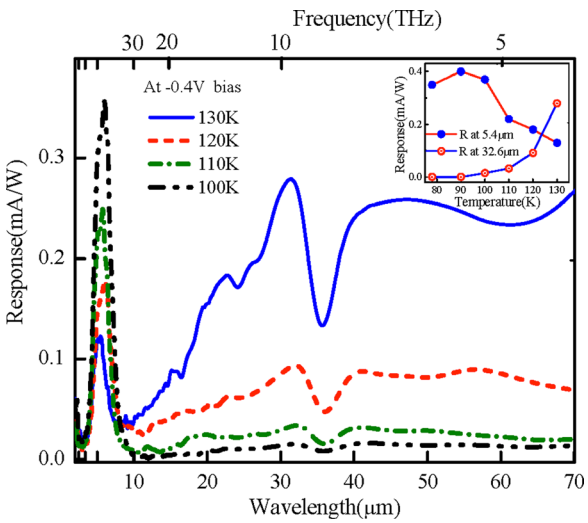

FIG. 3. The variation of MIR and THz response spectra with temperature at a fixed applied bias of −0.4 V. As the temperature increases, carriers are excited to higher levels reducing the rate of transitions that give rise to MIR response, whereas it enhances lower energy transitions or THz responses. The inset shows comparison of MIR and THz responses variation with temperature.

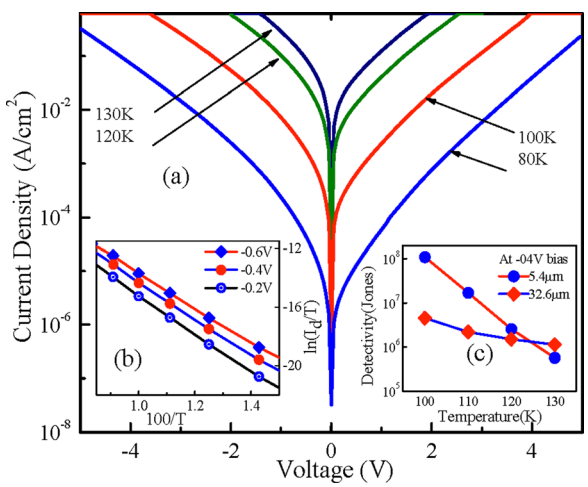

FIG. 4. (a) Variation of dark current density as a function of bias at different temperatures. (b) The Arrhenius plot of dark current to temperature ratio versus inverse temperature (100/T) for bias voltages of −0.2 V, −0.4 V, and −0.6 V. (c) Temperature variations of specific detectivity at 5.4 μm and 32.6 μm.

temperature (I_d/T) ratio versus inverse temperature (100/T) plot was found to be linear for the temperature range from ~60 K to ~130 K. At the bias voltage range from −0.2 V to −0.6 V, nearly the same activation energy as determined from the Arrhenius plot is ~108 meV. The exponential behavior observed in dark current indicates that carrier thermal excitation to higher energy states is possible and confirms the dominant role of thermionic emission in THz response.

The specific detectivity (D*) is calculated from the measured peak responsivity R_p and the noise density spectra i_n at different temperature and bias voltage using the relation $D^* = R_p\sqrt{Ax\Delta f}/i_n$, where A is the detector area and Δf is the frequency band width. The dark current noise density i_n was measured with low-noise voltage preamplifiers and a SRS 760 fast Fourier transform spectrum analyzer. The value of D* calculated for 5.4 μm absorption peak is 1.3×10^9 Jones at 78 K (−0.8 V bias) and 2.7×10^5 Jones at 130 K (−0.4 V bias). As shown in Figure 4(c), at 9.2 THz absorption peak, 130 K, and −0.4 V, the D* value is 1.4×10^6 Jones. Significant improvement can be achieved by using a double barrier resonant tunneling heterostructure, which suppresses most of the dark current without blocking the photocurrent.[13] The low dark current enhances detectivity and operates at high temperatures. Optimization of the number and density of QDs will also enhance the absorption. The other concern regarding p-type carriers is lower mobility as compared to electrons. Since the dot layer is thinner, the hole mobility mainly depends on the GaAs barrier. Optimizing thickness of the GaAs barrier between the dot layers can prevent multiple defects throughout the structure and enhances the photocurrent.

In conclusion, in addition to *p*-type MIR ($\lambda_p \sim 5.4\ \mu$m) detector at 78 K, we report a *p*-type THz (broad response with a peak response at ~9.2 THz) detector based on intersubband transitions in InAs/InGaAs DWELL structures. MIR peaks are associated with transitions from ground state of QD to continuum states, whereas the THz responses are originated due to higher temperatures (~100 K–130 K) and possibly to transitions between excited QD levels, bound-to-quasi-bound or continuum states. Therefore, detector response was extended to THz range up to ~4.28 THz (~70 μm) at a highest operating temperature of 130 K. Further optimization, such as doping level, width of the well, barrier thickness, using double barrier tunneling heterostructure or a thin dark current blocking layer reduces dark current, could enhance and extend the response of terahertz detection at temperature higher than 130 K, and improves detectivity.

This work was supported in part by the U.S. National Science Foundation under Grant No. ECCS-1232184. The Shanghai group acknowledges supports from the 863 Program of China (2011AA010205) and the Natural Science Foundation of China (91221201, 61234005, and 11074167). Financial support provided by The Center for Diagnostics and Therapeutics, to Fellowship of Georgia State University, Atlanta, Georgia, USA are also acknowledged.

[1]H. C. Liu, M. Gao, J. McCaffrey, Z. R. Wasilewski, and S. Fafard, Appl. Phys. Lett. **78**, 79 (2001).
[2]L. Jiang, S. S. Li, N.-T. Yeh, J.-I. Chyi, C. E. Ross, and K. S. Jones, Appl. Phys. Lett. **82**, 1986 (2003).
[3]S. Chakrabarti, A. D. Stiff-Roberts, X. Su, P. Bhattacharya, G. Ariyawansa, and A. G. U. Perera, J. Phys. D: Appl. Phys. **38**, 2135 (2005).
[4]H. Lim, S. Tsao, W. Zhang, and M. Razeghi, Appl. Phys. Lett. **90**, 131112 (2007).
[5]A. L. Betz, R. T. Boreiko, B. S. Williams, S. Kumar, Q. Hu, and J. L. Reno, Opt. Lett. **30**, 1837 (2005).
[6]M. B. M. Rinzan, A. G. U. Perera, S. G. Matsik, H. C. Liu, Z. R. Wasilewski, and M. Buchanan, Appl. Phys. Lett. **86**, 071112 (2005).
[7]S. Krishna, S. Raghavan, G. von Winckel, A. Stintz, G. Ariyawansa, S. G. Matsik, and A. G. U. Perera, Appl. Phys. Lett. **83**, 2745 (2003).
[8]G. Huang, W. Guo, P. Bhattacharya, G. Ariyawansa, and A. G. U. Perera, Appl. Phys. Lett. **94**, 101115 (2009).
[9]G. Ariyawansa, A. G. U. Perera, G. S. Raghavan, G. von Winckel, A. Stintz, and S. Krishna, IEEE Photonics Technol. Lett. **17**, 1064 (2005).
[10]A. V. Barve, S. Sengupta, J. O. Kim, Y. D. Sharma, S. Adhikary, T. J. Rotter, S. J. Lee, Y. H. Kim, and S. Krishna, Appl. Phys. Lett. **99**, 191110 (2011).
[11]B. F. Levine, J. Appl. Phys. **74**, R1–R81 (1993).
[12]J. R. Hoff, M. Razeghi, and G. J. Brown, Phys. Rev. B **54**, 10773 (1996).
[13]X. H. Su, J. Yang, P. Bhattacharya, G. Ariyawansa, and A. G. U. Perera, Appl. Phys. Lett. **89**, 031117 (2006).
[14]P. Bhattacharya, X. Su, S. Chakrabarti, G. Ariyawansa, and A. Perera, Appl. Phys. Lett. **86**, 191106 (2005).
[15]H. Jiang and J. Singh, Phys. Rev. B **56**, 4696 (1997).
[16]S. L. Chuang, *Physics of Optoelectronics Devices* (Wiley, New York, 1995).
[17]K. Sanjay, J. Phys. D: Appl. Phys. **38**, 2142 (2005).
[18]Y.-F. Lao, S. Wolde, A. G. U. Unil Perera, Y. H. Zhang, T. M. Wang, H. C. Liu, J. O. Kim, T. Schuler-Sandy, Z.-B. Tian, and S. S. Krishna, Appl. Phys. Lett. **103**, 241115 (2013).
[19]B. Kochman, A. D. Stiff-Roberts, S. Chakrabarti, J. D. Phillips, S. Krishna, J. Singh, and P. Bhattacharya, IEEE J. Quantum Electron. **39**(3), 459–467 (2003).
[20]A. G. U. Perera, W. Z. Shen, S. G. Matsik, H. C. Liu, M. Buchanan, and W. J. Schaff, Appl. Phys. Lett. **72**, 1596 (1998).
[21]M. R. Matthews, R. J. Steed, M. D. Frogley, C. C. Phillips, R. S. Attaluri, and S. Krishna, Appl. Phys. Lett. **90**, 103519 (2007).
[22]S. D. Gunapala, S. V. Bandara, C. J. Hill, D. Z. Ting, J. K. Liu, S. B. Rafol, E. R. Blazejewski, J. M. Mumolo, S. A. Keo, S. Krishna, Y. C. Chang, and C. A. Shott, Infrared Phys. Technol. **50**, 149 (2007).
[23]G. Huang, J. Yang, P. Bhattacharya, G. Ariyawansa, and A. G. U. Perera, Appl. Phys. Lett. **92**, 011117 (2008).